Eur Radiol (2013) 23:2546–2554
DOI 10.1007/s00330-013-2849-3

HEPATOBILIARY-PANCREAS

Contrast-enhanced ultrasound features of histologically proven focal nodular hyperplasia: diagnostic performance compared with contrast-enhanced CT

Wei Wang · Li-Da Chen · Ming-De Lu · Guang-Jian Liu · Shun-Li Shen · Zuo-Feng Xu · Xiao-Yan Xie · Yan Wang · Lu-Yao Zhou

Received: 1 January 2013 / Revised: 18 February 2013 / Accepted: 1 March 2013 / Published online: 27 April 2013

Abstract
Objectives To investigate and compare contrast-enhanced ultrasound (CEUS) in the characterisation of histologically proven focal nodular hyperplasia (FNH) with contrast-enhanced computed tomography (CECT).
Methods CEUS was performed in 85 patients with 85 histologically proven FNHs. Enhancement, centrifugal filling, spoke-wheel arteries, feeding artery and central scarring were reviewed and correlated with lesion size or liver background. Independent factors for predicting FNH from other focal liver lesions (FLLs) were evaluated. Forty-seven FLLs with CECT were randomly selected for comparison of diagnostic performance with CEUS.
Results Centrifugal filling was more common (P=0.002) and the significant predictor (P=0.003) in FNHs ≤3 cm. Lesion size or liver background has no significant influence on the detection rate of the spoke-wheel arteries and feeding artery (P>0.05). Central scarring was found in 42.6 % of FNHs ≥3 cm (P=0.000). The area under the ROC curve, sensitivity and specificity showed no significant differences between CEUS and CECT (P>0.05), except that the sensitivity of CEUS was better for reader 1 (P=0.041).
Conclusion CEUS is valuable in characterising centrifugal filling signs or spoke wheels in small FNHs and should be employed as the first-line imaging technique for diagnosis of FNH.
Key Points
- *The confident diagnosis of focal nodular hyperplasia is important in liver imaging.*
- *The centrifugal filling sign is useful for diagnosis of FNHs ≤3 cm.*
- *Contrast-enhanced ultrasound and contrast-enhanced CT have similar diagnostic performance for FNH.*
- *CEUS should be the first-line imaging technique for the diagnosis of FNH.*

Keywords Focal nodular hyperplasia · Contrast media · Contrast-enhanced ultrasound · Computed tomography · Diagnostic test

Abbreviations and acronyms

FNH	Focal nodular hyperplasia
FLLs	Focal liver lesions
CECT	Contrast-enhanced computed tomography
CEMRI	Contrast-enhanced magnetic resonance imaging
CEUS	Contrast-enhanced ultrasound
HCC	Hepatocellular carcinoma
ROC	Receiver-operating characteristic
Az	Area under the ROC curve

W. Wang · L.-D. Chen · M.-D. Lu · G.-J. Liu (✉) · Z.-F. Xu · X.-Y. Xie · Y. Wang · L.-Y. Zhou
Department of Medical Ultrasonics, The First Affiliated Hospital of Sun Yat-Sen University Institute of Diagnostic and Interventional Ultrasound, Sun Yat-Sen University, NO.58 Zhongshan Road 2, Guangzhou 510080, People's Republic of China
e-mail: guangjian1977@gmail.com

M.-D. Lu · S.-L. Shen
Department of Hepatobiliary Surgery, The First Affiliated Hospital of Sun Yat-Sen University, Guangzhou, China

PPV Positive predictive value
NPV Negative predictive value

Introduction

Focal nodular hyperplasia (FNH) is the second most common benign tumour of the liver, and the differentiation from other focal liver lesions (FLLs) is of great significance because of different managements and outcomes of the patients [1, 2]. Clinical diagnosis of FNH is often based on typical imaging findings on contrast-enhanced computed tomography (CECT) or magnetic resonance imaging (CEMRI); thus, histopathological confirmation is usually unnecessary [3, 4].

Contrast-enhanced ultrasound (CEUS) has been increasingly accepted as a technique comparable to CECT and CEMRI in the characterisation of FLLs [2, 3, 5–8]. Typical findings of FNH on CEUS include arterial hypervascularity, centrifugal filling, spoke-wheel arteries, feeding artery and hypoenhanced central scarring [5]. However, these findings are still not well documented owing to the small sample size and may not be easily identified in small FNHs according to the literature [7, 9–11]. For instance, the "spoke-wheel sign" is defined as spoke-wheel arteries with centrifugal filling, which follows the definition on colour Doppler ultrasound or angiography [12, 13]. This ambiguous definition would lead to misinterpretation of images and result in a variable detection rate of this typical finding from 27.3 % to 97.1 % [9–11, 14, 15].

Most previous studies concerning the CEUS findings of FNH have taken CECT and CEMRI to be the gold standard [4, 9, 14, 16–20]. It has been reported that early arterial phase (additional arterial phase) at CECT improves the differentiation of FNH from other FLLs [21], which is not essential in the standard imaging protocol because of the radiation hazard or acquisition time. Therefore, we presume that CEUS has the potential to provide more diagnostic information because of the advantage of high spatial and temporal resolution. In addition, although all three techniques are reported to be reliable for the diagnosis of FNH, none of these studies compared the diagnostic performance of CEUS and CECT [4, 6, 7, 20, 22].

The purpose of our study was to investigate the CEUS features of histologically proven FNH and compare the diagnostic performance of CEUS and CECT.

Materials and methods

Patient population

This retrospective study was approved by the institutional ethics committee, and informed consent was waived. Patients with FLLs were included in this study if they: *(1)* had undergone liver CEUS examination between March 2004 and June 2012 and (*2)* had histologically proven FNHs. The exclusion criteria were patients with *(1)* more than one type of disease, *(2)* cardiac insufficiency, *(3)* severe renal dysfunction and *(4)* pregnant women. Eighty-five patients (42 men and 43 women; mean age, 35 years±9 SD; range, 20–64 years) were included in this study, and a single lesion was selected in each patient. The pathological diagnosis was obtained by specimens from ultrasound-guided percutaneous biopsy (n=64) or surgical resection (n=21). Thirty-two (37.6 %), 50 (58.8 %) and 3 (3.5 %) lesions were located in the left, right and both lobes of the liver, respectively. Sixty-four (75.3 %) and 21 (24.7 %) lesions were located in normal and fatty liver, respectively. The size of lesions was 4.2 cm±2.7 SD (range, 1.1–15.3 cm), and the depth was 7.3 cm±2.7 SD (range, 3.0–16.0 cm).

CEUS techniques

Ultrasound examinations were performed using Acuson Sequoia 512 (Siemens Medical Solutions, Mountain View, CA, USA) equipped with a 4 V1 vector transducer (frequency range of 1.0 to 4.0 MHz) (n=45) or Aplio XV (Toshiba Medical Systems, Tokyo, Japan) equipped with a 375BT convex transducer (frequency range of 1.9 to 6.0 MHz) (n=40). Contrast-specific imaging (CSI) modes used in the present study were contrast pulse sequencing (mechanical index, MI, 0.15–0.21) and contrast harmonic imaging (MI, 0.05–0.08), respectively. After activation of the CSI mode, 2.4 ml of SonoVue (Bracco, Milan, Italy) was administered intravenously in a bolus fashion and flushed by 5 ml of 0.9 % saline solution. The target lesion was observed continuously for 6 min, and the entire arterial and portal phases and several repetitions of the late phase were stored on the hard disk. The arterial, portal and late phases were defined as 0–30 s, 31–120 s and 121–360 s after the injection, respectively. All the CEUS examinations were performed by three experienced radiologists (X.Z.F, L.G.J and X.X.Y., each with more than 8 years of experience in liver CEUS).

Image analysis

Two experienced radiologists (C.L.D and Z.L.Y with 5 years' experience in liver CEUS) randomly reviewed all the cine loops off-line on screen in consensus. Both readers had not been involved in the original examinations and were blinded to the final diagnosis, as well as to the clinical histories and other imaging findings of the patients. For each lesion, both readers were asked to document the following characteristic signs of FNH according to previous reports:

1. Enhancement: hyper-, iso- or hypo-enhancing, relative to the adjacent normal liver parenchyma [5, 19]
2. Centrifugal filling: initial central enhancement that progressed to the periphery of the lesion during the arterial phase [23]
3. Spoke-wheel arteries: arteries with a spoke-wheel or star-like morphology in the centre of the lesion during the arterial phase [9, 10, 19]
4. Feeding artery: hypertrophic artery directed towards the lesion and larger than the branches at the same depth during the arterial phase [9]
5. Central scar: stellate hypoenhanced linear or plicated area in the centre of the lesion during the portal or late phase [9, 19]

Both readers also evaluated and recorded the size, shape and echogenicity of lesions on baseline ultrasound and categorised the liver background as normal or fatty liver.

To determine whether centrifugal filling, spoke-wheel arteries, feeding artery and central scarring were important predictors for the characterisation of FNH, a multiple binary logistic regression model was used. In this model, in 85 historically proven FLLs (not FNH) with CEUS, which were randomly selected by using the sequence numbers, the above signs were also documented.

Comparison of the diagnostic performance of CEUS and CECT

Among 85 FNHs, 47 were analysed with CECT to compare the diagnostic performance of CEUS and CECT. During the same period (between March 2004 and June 2012), patients with proven pathological diagnosis of FLLs (not FNH) who underwent both CEUS and CECT served as a control group. In this group of patients, there were 26 hepatocellular carcinomas (HCC), 3 intrahepatic cholangiocarcinomas, 7 metastatic liver cancers, 1 combined hepatocellular carcinoma and cholangiocarcinoma, 3 haemangiomas, 2 focal fatty livers, 1 hepatic abscess, 1 infected granuloma, 2 cases of focal fibrosis after surgery and 1 atypical hyperplasia.

The CECTs in all patients were performed using 64-slice multidetector CT (Aquilion 64, Toshiba Medical System, Tokyo, Japan) within 1 month before or after CEUS examination. The standard dynamic contrast-enhanced scan procedure of our hospital is as follows: After an unenhanced helical sequence scan through the liver, 50–100 ml (1.5 ml/kg) of contrast agent (Ultravist 300, Schering, Berlin, Germany) was administered via antecubital vein at a rate of 3–4 ml/s. The arterial phase sequence was initiated 27 s after starting the injection, followed by a portal venous phase sequence beginning at 60 s. The following CT acquisition parameters were used: 120 kV, 200–250 mAs, collimation: 64 mm× 0.5 mm, slice thickness: 0.5 mm, slice increments: 0.5 mm and pitch: 0.9.

The CEUS digital images of FNHs and FLLs were randomly stored on a computer for analysis, and any identifying information (name, sex, and age) was concealed. Review was performed by two independent readers (X.Z.F and L.G.J). Both readers were blinded to patient identification, clinical history, other imaging results and pathological results. The diagnostic criteria for FNH at CEUS used in the present study were hyper-enhancement in the arterial phase without contrast washout in the portal or late phase, and with one or more typical features of centrifugal filling, spoke-wheel arteries, feeding artery and central scarring. Each reader used a subjective five-point scale to grade diagnostic confidence (grade 1=definitely FNH, grade 2=probably FNH, grade 3=indeterminate, grade 4=probably not FNH, grade 5=definitely not FNH).

All the CECT images were reviewed independently and retrospectively from a picture-archiving and communication system by two independent readers (X.Z.F and L.G.J, with more than 5 years of experience in CECT of the liver). Both readers were blinded to patient identification, clinical history, other imaging results and pathological results. The diagnostic criteria for FNH were determined according to previous literature [1, 4]. The same five-point scale for FNH diagnosis was used to grade diagnostic confidence.

For FNH diagnostic accuracy analysis of each technique, grades 1 and 2 were defined as positive results, and grades 3, 4 and 5 were defined as negative results.

Statistical analysis

All statistical analysis and the random sequence numbers were performed by using SPSS 16.0 software (SPSS Inc, Chicago, IL, USA). Data were presented as mean±standard deviation (SD) and percentage (%). $P<0.05$ was considered to indicate statistical significance. The association between lesion size or liver background and CEUS features of FNH was assessed using χ^2 or Fisher's exact test. Student's t test was used to compare lesion size within the same characteristic imaging findings. To investigate whether typical features were independent factors for predicting FNH, multiple binary logistic regression analysis was used. Weighted κ statistics were used to evaluate interreader agreement. The agreement was graded as follows: poor (κ<0.20), moderate (κ: 0.20 to<0.40), fair (κ: 0.40 to<0.60), good (κ: 0.60 to<0.80) or very good (κ: 0.80 - 1.00). Receiver-operating characteristic (ROC) curves of two imaging techniques were plotted and compared for evaluating the diagnostic performance of discrimination between FNHs and other FLLs using software (MedCalc version 9.0; MedCalc Software, Mariakerke, Belgium). The diagnostic performance was expressed as the area under the ROC curve (Az). Sensitivity, specificity, accuracy, positive

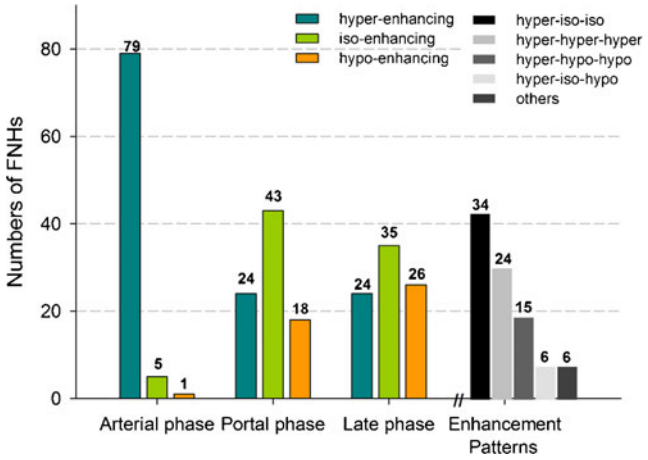

Fig. 1 *Bar graph* shows numbers of focal nodular hyperplasias (*FNHs*; on *top* of *bars*) with different enhancement levels in the arterial, portal and late phases (*colour bars*) and enhancement patterns (*greyscale bars*)

predictive value (PPV) and negative predictive value (NPV) were calculated. Differences in sensitivity and specificity were tested using the McNemar test.

Results

Enhancement in different vascular phases

The most common enhancement levels of FNH in the arterial, portal and late phases were hyper-enhancing (79/85, 92.4 %), iso-enhancing (43/85, 50.6 %) and iso-enhancing (35/85, 41.2 %), respectively (Fig. 1). The most common four enhancement patterns were "hyper-iso-iso" (34/85, 40.0 %), "hyper-hyper-hyper" (24/85, 28.2 %), "hyper-hypo-hypo" (15/85, 17.7 %) and "hyper-iso-hypo" (6/85, 7.1 %) (Fig. 1). No statistically significant differences were observed between lesion size or liver background and enhancement patterns (all $P>0.05$).

Typical features

For the 85 FNHs, centrifugal filling, spoke-wheel arteries, the feeding artery and central scarring were detected in 40 (47.1 %), 20 (23.5 %), 57 (67.1 %) and 20 (23.5 %), respectively (Table 1; Figs. 2, 3). Centrifugal filling was detected in 65.8 % of FNHs (25/38) measuring 3 cm or less in size and 31.9 % of FNHs larger than 3 cm (15/47; $P=0.002$). Central scarring was only found in 42.6 % of FNHs larger than 3 cm (20/47; $P=0.000$). No statistically significant differences were observed between the lesion size and detection rate of the spoke-wheel artery ($P=0.776$) or feeding artery signs ($P=0.621$). No statistically significant differences were observed between liver background and the detection rate of these typical features (all $P>0.05$; Table 1).

FNHs with signs of centrifugal filling were smaller than those without the sign (mean size: 3.1±1.5 cm vs. 5.2±3.2 cm, $P=0.000$; Fig. 4). However, FNHs with central scarring were larger than those without (mean size: 6.6±3.0 cm vs. 3.4±2.2 cm, $P=0.000$; Fig. 4). No significant difference was observed in the mean size of FNHs with and without spoke-wheel arteries ($P=0.574$) and the feeding artery ($P=0.965$; Fig. 4).

Analysis of independent factors for predicting FNH

All the typical features were found to be the independent factors for predicting FNHs at multiple logistic regression analysis. However, for lesions measuring 3 cm or less, only centrifugal filling was an independent feature for predicting FNH (Table 2), while for those larger than 3 cm, the feeding artery was not an independent factor (Table 2).

Comparison of the diagnostic performance of CEUS and CECT

The interreader agreement for the diagnosis of FNH based on a five-point scale was very good for CEUS and CECT (0.860±0.077 and 0.851±0.079, respectively). The diagnostic performance of the two techniques on FLLs in terms of Az, sensitivity, specificity, PPV, NPV and accuracy is shown in Table 3, and ROC curves are plotted in Fig. 5. For both readers, the Az, sensitivity and specificity of CEUS and CECT showed

Table 1 Typical features of focal nodular hyperplasias (FNHs) at contrast-enhanced ultrasound (CEUS): correlation with size and liver background

Typical CEUS features	Total (n=85)	Lesion size (cm)				P Value	Liver background		P value
		≤2.0 (n=13)	2.1-3.0 (n=25)	3.1-5.0 (n=23)	>5.0 (n=24)		Normal (n=64)	Fatty (n=21)	
Centrifugal filling	40 (47.1)	9 (69.2)	16 (64.0)	11 (47.8)	4 (16.7)	0.002	29 (45.3)	11 (52.4)	0.621
Spoke-wheel arteries	20 (23.5)	2 (15.4)	6 (24.0)	7 (30.4)	5 (20.8)	0.776	16 (25.0)	4 (19.0)	0.769
Feeding artery	57 (67.1)	9 (69.2)	19 (76.0)	15 (65.2)	14 (58.3)	0.621	42 (65.6)	15 (7.4)	0.790
Central scarring	20 (23.5)	0 (0.0)	0 (0.0)	9 (39.1)	11 (45.8)	0.000	17 (26.6)	3 (14.3)	0.376

Data are numbers of lesions, with percentages in parentheses

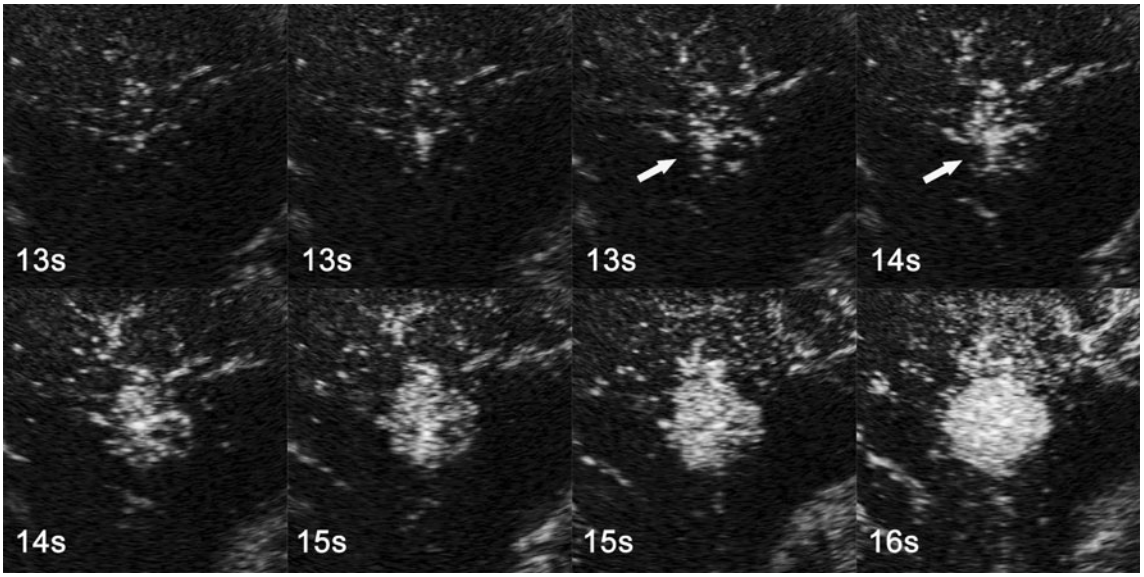

Fig. 2 Subcostal contrast-enhanced ultrasound (CEUS) images in a 24-year-old man with FNH (size=3.0 cm). Example shows that centrifugal filling with the spoke-wheel artery (*arrows*) sign is detected 13–16 s and 13–14 s after injection, respectively

no statistically significant differences (all $P>0.05$; Table 3), except for sensitivity for reader 1, which was 80.9 % (38/47) at CEUS versus 68.1 % (32/47) at CECT ($P=0.041$).

Diagnosis discordance between CEUS and CECT

Eight (nos. 01– 08) false-negative lesions were observed with no typical signs at CECT. However, these eight lesions presented centrifugal filling ($n=8$), spoke-wheel arteries ($n=3$) and the feeding artery ($n=7$) at CEUS (Table 4). The size of those lesions was 2.5±1.6 cm. One (no. 09) false-negative diagnosis was made by CEUS, which was shown as central scarring on CECT. There were five (nos. 10–14) false-positive diagnoses made by CEUS, with HCC in three, metastatic liver cancer in one and focal fibrosis after surgery in one. Among these lesions, centrifugal filling was detected (HCC, metastatic liver and focal fibrosis after surgery) in three, spoke-wheel arteries were detected (HCC and metastatic liver cancer) in two and the feeding artery was detected (HCC) in one.

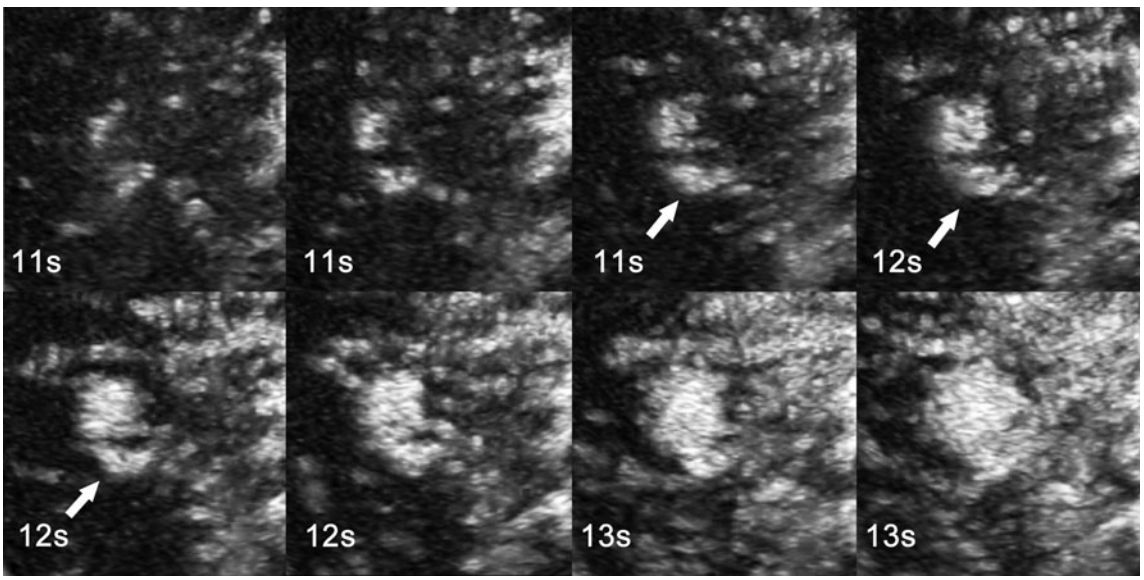

Fig. 3 Intercostal CEUS images in a 32-year-old woman with FNH (size=1.1 cm). Example shows that centrifugal filling without the spoke-wheel artery sign is detected 11–13 s after injection, and the feeding artery (*arrows*) is evident 11–12 s after injection

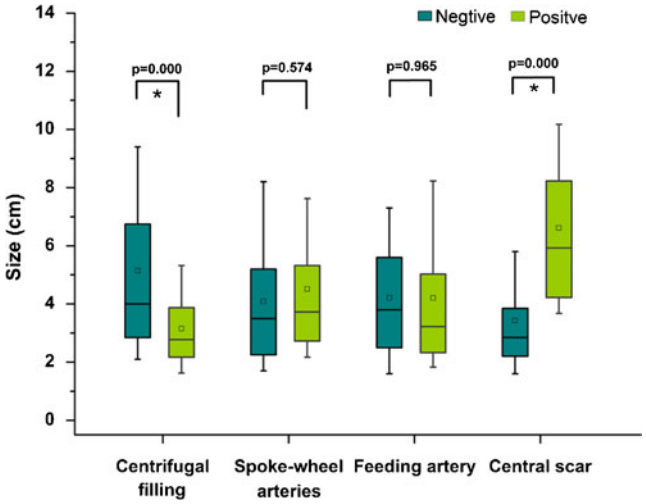

Fig. 4 Box plots of the size of FNHs with four additional signs. *Boxes*= range between 25th and 75th percentiles. *Horizontal line* in the *box*= median of size. □ = mean size. *Whiskers*=range between 10th and 90th percentiles. *Significant difference between lesions with positive and negative signs

Discussion

The typical enhancement pattern of FNHs at CEUS is generally accepted as hyper-enhancement in the arterial phase and hyper-/iso-enhancement in the portal and late phases [2, 5]. Contrast medium washout during the portal or late phase was reported at a rate of 3.3 % to 23.1 % [14, 17, 18]. In this group of FNHs with pathological confirmation, 68.2 % (58/85) of FNHs showed the typical enhancement pattern, but hypo-enhancement in the portal and late phase was detected in 21.2 % (18/85) and 30.6 % (26/85), respectively. In addition, 17.6 % (15/85) of FNHs even showed a typical malignant enhancement pattern of "hyper-hypo-hypo", which challenged the correct diagnosis [5]. Therefore, typical features are of great importance in the differentiation of FNH from other FLLs.

The "spoke-wheel sign" has been well documented in previous studies. Bartolotta et al. and Xu et al. reported a detection rate of 27.3–30.4 % [9, 11], whereas it dramatically increased to 92.3–97.1 % in other studies [10, 14]. Limitations of these studies are the small sample size and/or the lack of comparison with the histological diagnosis. Furthermore, the "spoke-wheel sign" referred to by these studies was defined as radial arterial centrifugal vascularity and enhancement at CEUS [9, 10, 17]. In our opinion, this ambiguous definition, including both the centrifugal filling and the spoke-wheel artery signs, would lead to misinterpretation of the images. In addition, micro-arteries of the "spoke-wheel sign" are difficult to detect in small lesions at CEUS (Fig. 3), owing to the relatively decreased spatial resolution on the contrast mode. Ungermann et al. reported the "spoke-wheel sign" to be detected in 30 % of lesions less than 3 cm and 17 % of those smaller than 2 cm [17].

To our knowledge, we investigated centrifugal filling and spoke-wheel arteries, which were shown in 47.1 % and 23.5 % of 85 FNHs, separately for the first time. Notably, the centrifugal filling sign was more common in FNHs measuring 3 cm or less, whereas there was no statistically significant difference observed between the lesion size and detection rate of the spoke-wheel arteries. Our findings were different from previous results that reported that the "spoke-wheel sign" has always been detected in larger FNHs [9, 10, 17]. The possible reasons could be because: *(1)* we emphasised the interpretation of the centrifugal filling sign instead of mixed findings of both centrifugal filling and spoke-wheel

Table 2 Multiple logistic regression analysis for independent factors for predicting FNH

Features	β Coefficient*	Odds ratio	95 % Confidence interval	*P* value
All (*n*=170)				
Centrifugal filling	2.093±0.450	9.905	4.097, 23.948	0.000
Spoke-wheel arteries	2.129±0.641	8.410	2.394, 29.543	0.001
Feeding artery	0.971±0.318	2.641	1.416, 4.925	0.002
Central scarring	1.829±0.572	6.231	2.029, 19.135	0.001
≤3 cm (*n*=64)				
Centrifugal filling	1.732±0.575	5.655	1.832, 17.455	0.003
Spoke-wheel arteries	1.088±0.837	2.968	0.575, 15.310	0.194
Feeding artery	1.014±0.536	2.758	0.965, 7.878	0.058
Central scarring	NA	NA	NA	NA
>3 cm (*n*=106)				
Centrifugal filling	3.114±1.055	22.500	2.846, 177.900	0.003
Spoke-wheel arteries	2.810±1.062	16.615	2.073, 133.151	0.008
Feeding artery	0.459±0.391	1.582	0.734, 3.407	0.241
Central scarring	2.107±0.593	8.226	2.572, 26.309	0.000

NA=data not available

*Values are means±standard errors

Table 3 Diagnostic performance of CEUS and CECT for both readers

Reader	Imaging technique	Az*	Sensitivity (%)†	Specificity (%)†	Positive predictive values (%)†	Negative predictive values (%)†	Accuracy (%)†
Total (n=94)							
Reader 1	CEUS	0.917 (0.842, 0.964)	80.9 (38/47)	95.7 (45/47)	95.0 (38/40)	83.3 (45/54)	88.3 (83/94)
	CECT	0.905 (0.827, 0.956)	68.1 (32/47)	95.7 (45/47)	94.1 (32/34)	75.0 (45/60)	81.9 (77/94)
	P Value	0.688	0.041	0.617	NA	NA	NA
Reader 2	CEUS	0.927 (0.854, 0.970)	78.7 (37/47)	93.6 (44/47)	92.5 (37/40)	81.5 (44/54)	86.2 (81/94)
	CECT	0.927 (0.854, 0.970)	70.2 (33/47)	97.9 (46/47)	97.1 (33/34)	76.7 (46/60)	84.0 (79/94)
	P Value	1.000	0.221	0.617	NA	NA	NA

*Data in parentheses are 95 % confidence intervals

†Data in parentheses are those used to calculate the percentages

arteries; *(2)* the gold standard of our study was histopathology. As FNHs with centrifugal filling were smaller than those without the finding, it consequently might be ignored if no spoke-wheel vascularity were detected in the lesion (Fig. 3) [10]. In previous studies [9, 16–18], the final diagnosis confirmed by CECT depends on static signs, such as enhanced intensity and central scarring. As central scarring could only be detected in relatively large FNHs, there must be many small FNHs that are excluded by the "gold standard". Therefore, the dynamic centrifugal filling and spoke wheel artery signs were inevitably missed. We found that the centrifugal filling sign was the only independent factor for predicting FNH measuring 3 cm or less, which is important for the differentiation of small FNHs from other FLLs.

Although the feeding artery sign was the most common sign of FNHs at CEUS, it showed the lowest odds ratio for characterisation of FNH, which indicates that it was also regularly observed in other FLLs. As for central scarring, a detection rate of 31.6 % to 63.3 % [3, 11, 17, 18] was reported, while our study demonstrated a lower rate of 23.5 % (Table 1). None of the FNHs smaller than 3 cm presented central scarring, which might explain the lower detection rate compared with other studies [18].

The diagnostic performance of CEUS on FLLs was reported to be equal to that of CECT [4, 6, 7, 20]. In two prospective multicentre studies, Seitz et al. evaluated the diagnostic performance of CEUS for the characterisation of FLLs compared with CECT or CEMRI [6, 7]. In the subgroup taking CECT as the reference standard, there were one and two discordance diagnoses for FNH, respectively. However, in the other histologically proven FNH group, they found sensitivity of CEUS and CECT reduced to 57.1 % and 42.9 %, respectively, and more discordance with CEUS [6, 7]. Until now, most studies of FNH at CEUS were based on CECT or CEMRI, and none of these studies was able to compare the diagnostic performance of CEUS and CECT [9, 14, 16–19, 24].

In our study, a very good interreader agreement was obtained for CEUS, which revealed good reproducibility of the diagnostic performance. The ROC analysis of our study confirmed that compared with CECT, CEUS showed equal diagnostic performance for both readers. Although the Az and specificity of CEUS and CECT showed no statistically significant difference, the sensitivity of CEUS (80.9 %) was better than that of CECT (68.1 %) for reader 1. Thus, considering the advantages of flexibility, availability, cost effectiveness and absence of radiation, characterisation of FNHs using CEUS would be of great clinical value.

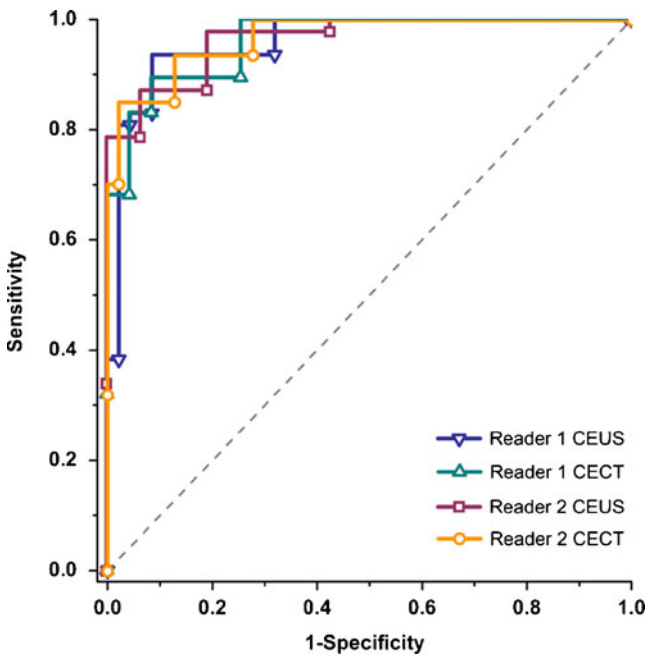

Fig. 5 Receiver-operating characteristic (*ROC*) curves show the diagnostic performance of CEUS compared with CECT in differentiating FNH from other focal liver lesions (*FLLs*). There was no statistically significant difference between CEUS and CECT for both readers (all P>0.05), and the *dashed line* represents reference values

Table 4 Discordant diagnosis of CEUS vs. CECT

Lesions	Reader	Diagnosis		Lesion size (cm)	Enhancement pattern	Typical features*				Histopathological diagnosis
		CEUS	CECT			Centrifugal filling	Spoke-wheel arteries	Feeding artery	Central scarring	
No. 01	Both	FNH	Not FNH	2.5	Hyper-iso-iso	+	-	+	-	FNH
No. 02	Both	FNH	Not FNH	1.7	Hyper-hypo-hypo	+	-	+	-	FNH
No. 03	Both	FNH	Not FNH	1.4	Hyper-iso-iso	+	+	+	-	FNH
No. 04	Both	FNH	Not FNH	5.9	Hyper-hypo-hypo	+	+	-	-	FNH
No. 05	Reader 1	FNH	Not FNH	2.2	Hyper-iso-iso	+	-	+	-	FNH
No. 06	Reader 1	FNH	Not FNH	4.0	Hyper-iso-iso	+	+	+	-	FNH
No. 07	Reader 2	FNH	Not FNH	1.1	Hyper-iso-iso	+	-	+	-	FNH
No. 08	Reader 2	FNH	Not FNH	1.1	Hyper-iso-iso	+	-	+	-	FNH
No. 09	Reader 2	Not FNH	FNH	4.5	Hyper-iso-iso	-	+	-	-	FNH
No. 10	Reader 1	FNH	Not FNH	2.2	Hyper-hypo-hypo	+	-	+	-	HCC
No. 11	Reader 1	FNH	Not FNH	2.4	Hyper-hypo-hypo	+	-	+	-	Focal fibrosis after surgery
No. 12	Reader 2	FNH	Not FNH	2.7	Hyper-hypo-hypo	-	+	+	-	HCC
No. 13	Reader 2	FNH	Not FNH	2.6	Hyper-hypo-hypo	+	+	+	-	Metastatic liver cancer
No. 14	Reader 2	FNH	Not FNH	2.5	Hyper-iso-iso	-	-	+	-	HCC
No. 15	Both	Not FNH	FNH	5.8	Hyper-hypo-hypo	-	-	+	-	HCC
No. 16	Reader 1	Not FNH	FNH	8.7	Hyper-hypo-hypo	-	-	+	-	HCC

*The symbolS "+" and "-" stand for positive and negative, respectively

Eight false-negative lesions (nos. 01–08) at CECT by both readers presented no diagnostic signs with a mean size of 2.5 cm, whereas in all lesions the centrifugal filling sign was detected at CEUS. We presume that CEUS might be better in the characterisation of small FNHs because dynamic signs may be missed at CECT. On the other hand, centrifugal filling and the spoke-wheel sign could also lead to misinterpretation in four false-positive lesions at CEUS (nos. 10–13). The other discrepancies between CEUS and CECT are probably due to: *(1)* better spatial resolution of CECT for the detection of central scarring and *(2)* personal experience, which cannot be excluded for the two imaging techniques.

Our study had some limitations. First, FNHs with obviously benign findings at imaging did not undergo biopsy or surgery, which may have resulted in a detection rate of CEUS features that is discordant with factual incidence. Second, the centrifugal filling sign has also been reported to be detected in hepatic adenoma [19], and it was detected in HCC, metastatic liver cancer and focal fibrosis after surgery in our study. Therefore, a more specific control group should be selected to verify the importance of this sign in the characterisation of small FNHs. Third, the cases in the diagnostic test of CEUS and CECT were limited, which may have influenced the accuracy of the two techniques.

In conclusion, CEUS is superior to CECT for characterising dynamic centrifugal filling or the spoke-wheel sign in small lesions. With similar diagnostic performance to CECT, CEUS should be employed as the first-line imaging technique for the diagnosis of FNH, taking into consideration radiation exposure and cost effectiveness.

Acknowledgements Our work is supported by the National Natural Science Foundation of China (no. 30901384, 81271576).

References

1. Hussain SM, Terkivatan T, Zondervan PE et al (2004) Focal nodular hyperplasia: findings at state-of-the-art MR imaging, US, CT, and pathologic analysis. Radiographics 24:3–17
2. Dietrich CF, Maddalena ME, Cui XW, Schreiber-Dietrich D, Ignee A (2012) Liver tumor characterization–review of the literature. Ultraschall Med 33:S3–S10
3. Quaia E, Calliada F, Bertolotto M et al (2004) Characterization of focal liver lesions with contrast-specific US modes and a sulfur hexafluoride-filled microbubble contrast agent: diagnostic performance and confidence. Radiology 232:420–430
4. Burns PN, Wilson SR (2007) Focal liver masses: enhancement patterns on contrast-enhanced images–concordance of US scans with CT scans and MR images. Radiology 242:162–174
5. Claudon M, Cosgrove D, Albrecht T et al (2008) Guidelines and good clinical practice recommendations for contrast enhanced ultrasound (CEUS) - update 2008. Ultraschall Med 29:28–44
6. Seitz K, Bernatik T, Strobel D et al (2010) Contrast-enhanced ultrasound (CEUS) for the characterization of focal liver lesions in clinical practice (DEGUM Multicenter Trial): CEUS vs. MRI–a prospective comparison in 269 patients. Ultraschall Med 31:492–499
7. Seitz K, Strobel D, Bernatik T et al (2009) Contrast-enhanced ultrasound (CEUS) for the characterization of focal liver lesions—prospective comparison in clinical practice: CEUS vs. CT (DEGUM multicenter trial). Parts of this manuscript were presented at the Ultrasound Dreilandertreffen 2008, Davos. Ultraschall Med 30:383–389
8. Dietrich CF (2012) Liver tumor characterization—comments and illustrations regarding guidelines. Ultraschall Med 33:S22–S30
9. Bartolotta TV, Taibbi A, Matranga D, Malizia G, Lagalla R, Midiri M (2010) Hepatic focal nodular hyperplasia: contrast-enhanced ultrasound findings with emphasis on lesion size, depth and liver echogenicity. Eur Radiol 20:2248–2256
10. Yen YH, Wang JH, Lu SN et al (2006) Contrast-enhanced ultrasonographic spoke-wheel sign in hepatic focal nodular hyperplasia. Eur J Radiol 60:439–444
11. Xu HX, Liu GJ, Lu MD et al (2006) Characterization of focal liver lesions using contrast-enhanced sonography with a low mechanical index mode and a sulfur hexafluoride-filled microbubble contrast agent. J Clin Ultrasound 34:261–272
12. Rogers JV, Mack LA, Freeny PC, Johnson ML, Sones PJ (1981) Hepatic focal nodular hyperplasia: angiography, CT, sonography, and scintigraphy. Am J Roentgenol 137:983–990
13. Wang LY, Wang JH, Lin ZY et al (1997) Hepatic focal nodular hyperplasia: findings on color Doppler ultrasound. Abdom Imaging 22:178–181
14. Kim MJ, Lim HK, Kim SH et al (2004) Evaluation of hepatic focal nodular hyperplasia with contrast-enhanced gray scale harmonic sonography: initial experience. J Ultrasound Med 23:297–305
15. Liu GJ, Wang W, Xie XY et al (2010) Real-time contrast-enhanced ultrasound imaging of focal liver lesions in fatty liver. Clin Imaging 34:211–221
16. Piscaglia F, Venturi A, Mancini M et al (2010) Diagnostic features of real-time contrast-enhanced ultrasound in focal nodular hyperplasia of the liver. Ultraschall Med 31:276–282
17. Ungermann L, Elias P, Zizka J, Ryska P, Klzo L (2007) Focal nodular hyperplasia: spoke-wheel arterial pattern and other signs on dynamic contrast-enhanced ultrasonography. Eur J Radiol 63:290–294
18. Dietrich CF, Schuessler G, Trojan J, Fellbaum C, Ignee A (2005) Differentiation of focal nodular hyperplasia and hepatocellular adenoma by contrast-enhanced ultrasound. Br J Radiol 78:704–707
19. Kim TK, Jang HJ, Burns PN, Murphy-Lavallee J, Wilson SR (2008) Focal nodular hyperplasia and hepatic adenoma: differentiation with low-mechanical-index contrast-enhanced sonography. Am J Roentgenol 190:58–66
20. Guang Y, Xie L, Ding H, Cai A, Huang Y (2011) Diagnosis value of focal liver lesions with SonoVue(R)-enhanced ultrasound compared with contrast-enhanced computed tomography and contrast-enhanced MRI: a meta-analysis. J Cancer Res Clin Oncol 137:1595–1605
21. Van Hoe L, Baert AL, Gryspeerdt S et al (1997) Dual-phase helical CT of the liver: value of an early-phase acquisition in the differential diagnosis of noncystic focal lesions. Am J Roentgenol 168:1185–1192
22. Wilson SR, Kim TK, Jang HJ, Burns PN (2007) Enhancement patterns of focal liver masses: discordance between contrast-enhanced sonography and contrast-enhanced CT and MRI. AJR Am J Roentgenol 189:W7–W12
23. Kudo M, Tomita S, Tochio H, Kashida H, Hirasa M, Todo A (1991) Hepatic focal nodular hyperplasia: specific findings at dynamic contrast-enhanced US with carbon dioxide microbubbles. Radiology 179:377–382
24. Strobel D, Bernatik T, Blank W et al (2011) Diagnostic accuracy of CEUS in the differential diagnosis of small (</= 20 mm) and subcentimetric (</= 10 mm) focal liver lesions in comparison with histology. Results of the DEGUM multicenter trial. Ultraschall Med 32:593–597